EGTRIB Journal
JOURNAL OF
THE EGYPTIAN SOCIETY OF TRIBOLOGY
VOLUME 20, No. 3, July 2023, pp. 23 - 39 **ISSN 2090 - 5882**
(Received February 07. 2023, Accepted in final form April 27. 2023) **jest.journals.ekb.eg**

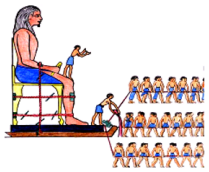

INVESTIGATION OF MECHANICAL AND TRIBOLOGICAL PROPERTIES OF THE PTFE/PA12 POLYMERIC DUAL-MATRIX REINFORCED WITH ZnO NPs FOR PROSTHETICS APPLICATIONS.

Hassan A. El-Sayed M., El-Sheikh M. N., Rohim M. Nafea M.

[1]**Production Technology Dept., Faculty of Technology and Education, Beni-Suef University, Beni-Suef, EGYPT.**

ABSTRACT

The current study aims to introduce novel nanocomposites consisted of polymeric dual-matrix, polytetrafluorethylene/polyamide12 (PTFE/PA12), reinforced with zinc oxide nanoparticles (ZnO NPs) for prosthetics applications. PA12 content to polymeric dual-matrix was 5, 10, 15, and 20 weight fraction (wt. %). Also, ZnO NPs, which were characterized by transmission electron microscope (TEM), were filled into the dual-matrix of PTFE/PA12 by 0.25, 0.5, 1, and 1.5 wt. %. All the present nanocomposites were fabricated by a hot-pressing technique. Compression, microhardness, wear, and friction tests were performed to study the mechanical and tribological properties of all the fabricated nanocomposites. After the wear test, worn surfaces were examined by scanning electron microscope (SEM) to emphasize the occurred wear mechanism.

Experimental results revealed that the optimum content of PA12 and ZnO NPs into proposed nanocomposites were 15 and 1 wt. %, respectively. Consequently, elastic modulus, compressive yield strength, Vickers hardness number (VHN), wear rate and friction coefficient of PTFE/15 wt. % PA12, as a dual-matrix, were enhanced by 125.48, 70.88, 81.68, 57.27, and 54.16 %, respectively compared to pure PTFE. Also, elastic modulus, compression yield strength, VHN, wear rate, and friction coefficient of the proposed PTFE/15 wt. %/1 wt. % ZnO NPs composite showed significant improvements by 51.58, 58.59, 50.86, 73.91, and 44.63%, respectively compared to the pure dual-matrix. Worn surfaces of the proposed composites proved that a significant enhancement was observed compared to the other worn surfaces. According to that, the proposed nanocomposites of PTFE/15 wt. % PA12/1 wt. % ZnO NPs are considered as a suitable choice for prosthetic applications.

KEYWORDS

Wear rate, friction coefficient, Vickers hardness number, compressive yield strength, elastic modulus.

INTRODUCTION

Polymeric biomaterials have been developed at many fields such as, biology, chemistry, materials, physics, and medicine, [1, 2]. Polymers have been applied to a wide range of biomedical applications such as implants, surgical, and orthopedic ones. The widespread application of biomedical polymers because of their biological, physical, and chemical properties such as the affordable price, flexibility, ease of manufacturing, [3, 4]. It is noticed that some polymers satisfy the tribological requirements; but, in the hybrid and composite forms, they often have more advantages, [5]. So, many researchers studied the improvement of functional and structural characteristics of hybrid materials such as nanocomposite-based polymers. The hybrid materials could be inorganic and organic nanofillers with size of ≤ 100 nm, [6].

Nanofillers include metals, carbon nanotubes, ceramics, silicates, and metal oxides. Hence, composites fabrication requires an understanding of the nanostructures to be used in the desired application. The main changes of the new composites is the mechanical and functional features so controlling the interaction, ratio, nanofiller size, and temperature of the interaction resulted on new property nanocomposites, [7, 8]. This combination could be inserted into various requirements, [9].

Current lubrication systems based on the use of mineral or lubrication oil that cannot be used in health care fields such as pharmaceutical, and food industries to prevent the product contamination, [10]. In this regard, liquid lubricants could be replaced by solid lubricants to control wear and friction. However, solid lubricants must have certain requirements in practical applications, such as stiffness, thermal expansion, mechanical strength, damping, and fatigue life, [11].

One important used solid lubricant is polymers, which used as solid lubricant in mechanical parts due to their important properties such as excellent wear, light weight, solvent resistance, and high strength, [12]. PTFE, named "Teflon," has extremely well chemical resistance, and low friction coefficient, [13, 14]. Also, PTFE has hydrophobic, low friction coefficient anti-stiction, and biocompatible properties, [15]. However, its disadvantage is the poor wear resistance. Therefore, to improve its properties, NPs, [16], and fibrous fillers (whisker, carbon fiber, and glass fiber), [17, 18] could be added into PTFE. So, it could be used as a filler with other polymers to enhance their tribological properties, [19, 20].

Polymer composites are used in the engineering industry because of their high impact strength and tensile. Among the used plastic materials is the polyamides because of their low cost, and well mechanical features, [21]. PAs have semi-crystalline structure, the crystalline areas increase their yield strength, rigidity, melt temperature, creep resistance, and chemical resistance. Besides that, amorphous regions affect PAs permeability, impact resistance, elastic properties, and thermal expansion. However, PAs are hydroscopic so moisture affects PAs features, [22]. Moisture affects PAs yield stress and elastic modulus, but it increases their elongation and flexibility. Moreover, humidity affects PAs end-use performance and processing, [23]. In general, humidity could affect composite structures. Hence, water must be removed from PAs by

thermal processing to prevent affecting the composite mechanical properties and hydrolytic degradation, [24].

PA 12 has good properties so when combined with other polymers, it can improve the performance especially by adding NPs. PA 12 has great interest because of its barrier properties, wear resistance, and high strength, [25]. But it has some disadvantages of sensitivity to humidity, which affects its mechanical characteristics and stability. Also, it has poor heat conductivity, [21, 26]. Herein, PA 12 has been involved in composites to sacrifice its mechanical characteristics to be applied into industrial applications, [27]. Nevertheless, they could be applied in many industries such as gear and bearings. It was found that 56 wt.% of polyphenylene sulfide (PPS) composite by adding polyamide 66 (PA) 24 wt.% and PTFE 24 wt.% showed the best tribological properties, [28].

Polymer-based nanofillers have been widely used due to their unique thermal, electrical, frictional, catalytic, and mechanical properties as fillers, [29]. Among those nanofillers is ZnO NPs, [30], which have important advantages such as nontoxicity, and antimicrobial nature, its unique electrochemical, optical, and electronic properties, [31]. So, ZnO NPs have been used as a reinforcement nano-filler in many polymers including polymethylmethacrylate (PMMA), [32], ultrahigh molecular weight polyethylene (UHMWPE), [33], polyurethane (PU), [34], PTFE, [35, 36], and polyetheretherketone (PEEK), [37].

Xu *et al*. showed that PA6/ZnO composite with 0.2% ZnO NPs had little effect on the impact strength of PA6, while it enhanced the tensile enhanced by 75%, [38]. Also, Li *et al*., [36] reported that the wear volume loss of 15 vol.% ZnO filled in PTFE compared to pure PTFE is only 1%. Chang *et al*., [33] reported that 10 wt.% ZnO NPs/UHMWPE reached the best wear resistance and compressive strength compared to the pure UHMWPE. However, Saeed *et al*. proved that 30% ZnO/nylon 6/6 nanocomposite mechanical properties are decreased than the neat polymer due to ZnO NPs agglomeration, [39].

Some polymeric nanocomposites could be applied to prosthetic applications. It was shown that multi-walled carbon nanotube (WMCNT)/natural rubber (NR) polymer nanocomposite could be applied for prosthetic foot, [40]. Also, high-density polyethylene (HDPE)/MWCNT/Alumina NPs was selected to be applied for artificial joints, [41]. Ce-TZP/Al_2O_3 nanocomposites were manufactured to be applied to denture prosthetics, [42].To sum up, no prior work has been done on fabrication of PTFE/PA 12/ZnO NPs composites. Therefore, this work focused on studying the mechanical and tribological properties of these nanocomposites to be applied on prosthetic application.

MATERIALS AND EXPERIMINTS

Materials

A commercial powdered PTFE, has a size of 200 µm, was used as the first component of the dual -matrix material, while the second one is the powdered PA 12, which is supplied by EOS Company, North America, with an average size of 22.3 nm. ZnO NPs, with an average size of 20 ± 5 nm, were supplied from NANOTECH Company,

Egypt, as shown in Fig. 1 a. They were used as reinforcement material for dual-matrix.

Samples Preparation

In this work, the nanocomposites were prepared using hot pressing technique based on the experimental work steps that indicated in Fig. 1 b. PA12 to PTFE was 0, 5, 10, 15, and 20 wt. % to obtain the dual-matrix of PTFE/PA12. ZnO NPs were added to each dual-matrix by 0, 0.25, 0.5, 1, and 1.5 wt. %. Therefore, twenty-five samples were prepared as shown in Table 1. PTFE/PA12 with various contents of 0, 0.25, 0.5, 1, and 1.5 wt. % ZnO NPs were mixed in agate mortar continuously to obtain the homogenous composites. After that, the mixed composites were put into a cylindrical hot-working steel pressing die, Fig. 2, which was 6.5 mm in diameter. The composite was pressed inside the pressing die at a pressure of four bars for five minutes after the temperature reached 150 ºC, [43]. A cooling fan was used to facilitate the sample solidification with the final shape of 6.5 mm in diameter and 30 mm in length. Finally, all specimens were cut into suitable dimensions and prepared for further tests.

Testing and Characterization

Samples were prepared to examine the mechanical and tribological properties of the present PTFE/PA12/ZnO NPs composites. Mechanical properties include the compression and Vickers hardness tests. The compression test was conducted at room temperature (35 ± 5 ºC) using SHIMADZU universal testing machine (UH series). Three samples were prepared at each filler content according to ASTM D695 and the machine cross head speed was 5 mm/min. Engineering stress-strain curves of the tested samples were automatically plotted and recorded on the testing machine computer. After that, the elastic modulus was calculated from engineering stress-strain curve slope of each sample.

The specimens were cut and polished for Vickers hardness test with a diameter of 6.5 mm and length of 10 mm. Vickers hardness test was performed at room temperature (35 ± 5 ºC) based on the ASTM E384-99. The specimens dwelled under the indenter load of 50 g for up to 10 s. The occurred indentations were measured by a light microscope mounted on the testing machine. The hardness number was calculated by dividing the applied load by the square of mean diagonal of the indentation. To obtain more accurate results, at least five indentations of each three samples were taken at different places on the specimen surface, and the average value was estimated.

Tribological properties, which include wear rate and friction coefficient tests were performed via pin-on-disk tribometer test rig upon ASTM standard G99, [44]. Fig. 3 indicates a schematic of pin-on-disk tribometer test rig used for sliding wear experiments. The specimens were cut and prepared as a pin shape with dimensions of 6.5 and 30 mm in diameter and length, respectively. All nanocomposites were tested under dry sliding conditions, at room temperature (35 ± 5 ºC), against carbon steel disk counterface at constant testing conditions of applied normal load, sliding distance, and sliding speed of 30 N, 212 m, and 1.2 m/s, respectively.

Alumina abrasive paper with a grade of 1000 grit (Ra = 4.6 mm) was glued onto a counterface disk, [45]. Before and after the wear test, specimens were weighed on an electronic balance which has ± 0.1 mg accuracy, and the difference between the two

weights represents the wight loss. Wear rate was calculated by dividing the weight loss by sliding distance. For each specimen composition, the wear tests were repeated at least three times and the averaged values were reported.

At the same wear test conditions, friction forces were measured and recorded each one millisecond by a load cell, which connected with a data logger system. By dividing the averaged friction forces by the applied load, the friction coefficient was estimated. Friction coefficient was measured at least three times for each specimen and the averaged value was considered.

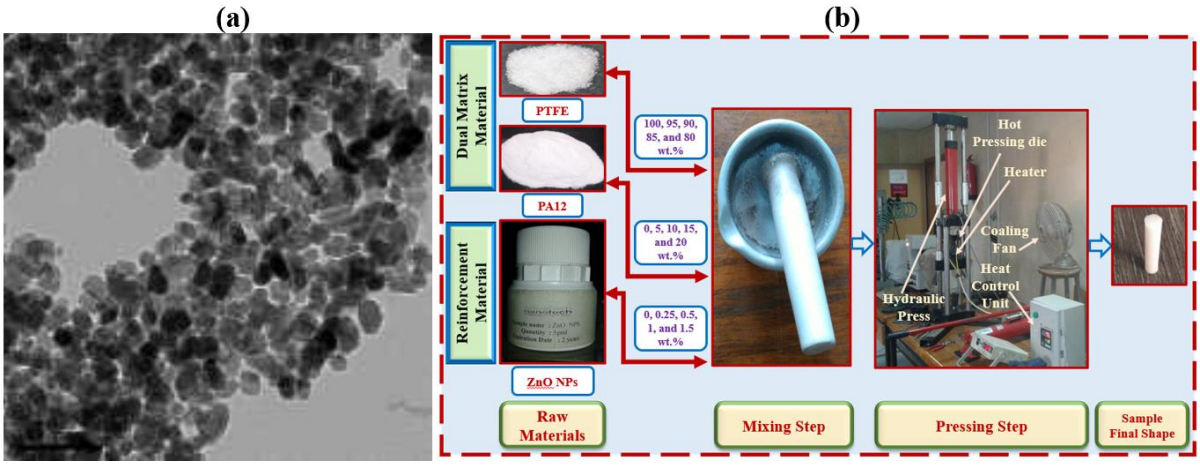

Fig. 1, a TEM image of ZnO NPs, b): Experimental work steps.

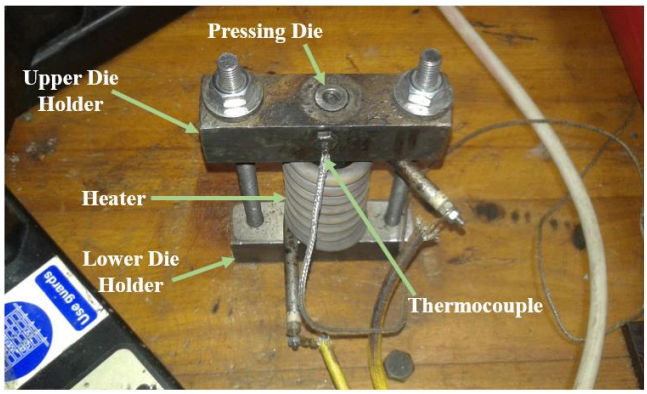

Fig. 2 Hot-working steel pressing die.

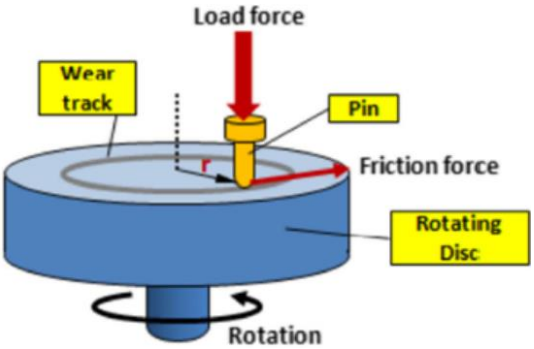

Fig. 3 Schematic of a pin-on-disk tribometer test rig, [46].

Table 1 Specimens composition

Specimen No.	Specimen Composition		
	Dual-Matrix		ZnO NPs, wt.%
	PTFE, wt.%	PA12, wt.%	
1	100	0	0
2	99.75	0	0.25
3	99.5	0	0.5
4	99	0	1
5	98.5	0	1.5
6	95	5	0
7	94.75	5	0.25
8	94.5	5	0.5
9	94	5	1
10	93.5	5	1.5
11	90	10	0
12	89.75	10	0.25
13	89.5	10	0.5
14	89	10	1
15	88.5	10	1.5
16	85	15	0
17	84.75	15	0.25
18	84.5	15	0.5
19	84	15	1
20	83.5	15	1.5
21	80	20	0
22	79.75	20	0.25
23	79.5	20	0.5
24	79	20	1
25	78.5	20	1.5

RESULTS AND DISSCUSION

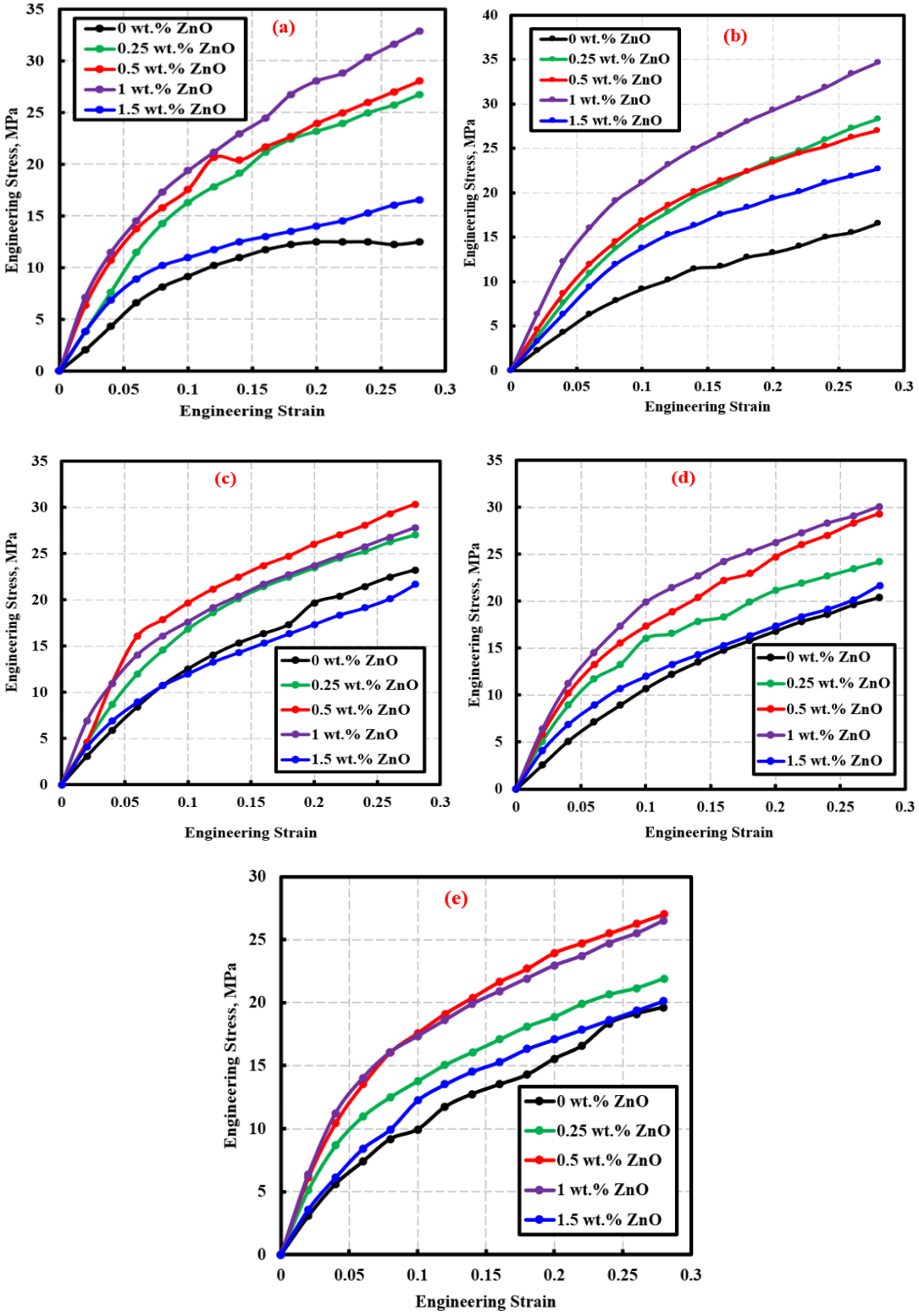

Fig. 3 Engineering stress-strain curves a): PTFE/0 wt. % PA12/ZnO NPs, b): PTFE/5 wt. % PA12/ZnO NPs, c): PTFE/10 wt. % PA12/ZnO NPs, d): PTFE/15 wt. % PA12/ZnO NPs, and e): PTFE/20 wt. % PA12/ZnO NPs.

Figure 3 indicates the engineering stress-strain curves of the present PTFE/PA12/ZnO composites, which were obtained by the compression test. These curves are characterized by a region of linear elasticity followed by a region of yield and plastic deformation. Therefore, the behavior of the present nanocomposites under compression load contributes to estimate the modulus of elasticity and yield strength. The elastic modulus and compressive yield strength of PTFE were enhanced by increasing PA12 content up to 15 wt. %, as indicated in Figs 4 and 5, respectively. Also, the elastic modulus after adding ZnO NPs content of 0.25, 0.5, 1, and 1.5 wt. % was improved by 6.65, 15.49, 51.58, and 17.64 %, respectively compared to PTFE/15 wt. % PA12, as shown in Fig. 4. As indicated in Fig. 5, the compressive yield strength of PTFE/15 wt. % PA12 composites was increased by 37.77, 51.03, 58.58, and 5.7 % at 0.25, 0.5, 1, and 1.5 wt. % ZnO NPs, respectively. These improvements indicate that the nanofillers have an effective role in improving the ductile performance of PTFE/PA12 matrix composites, [47].

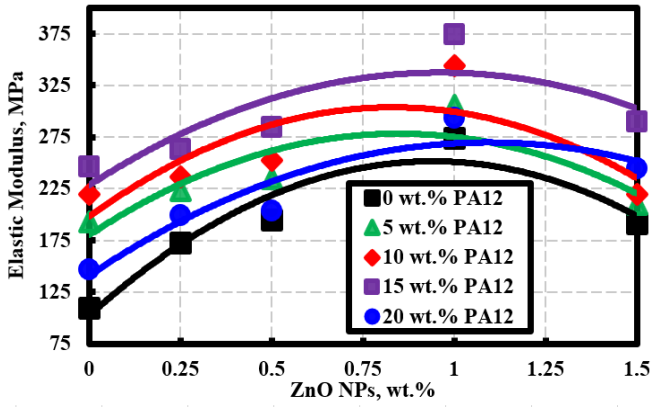

Fig. 4 Elastic modulus of the present.

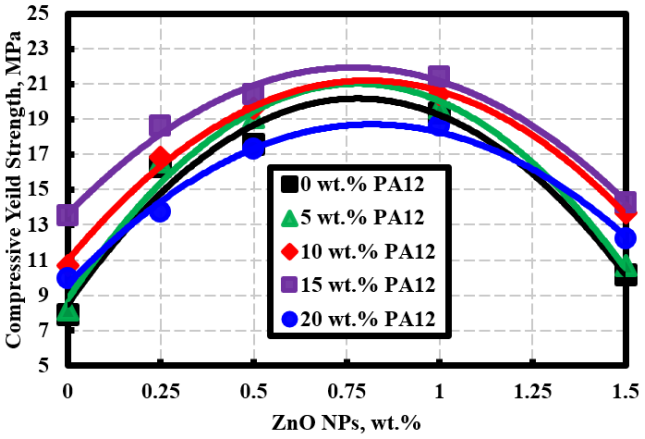

Fig. 5 Compressive yield strength of the present nanocomposites.

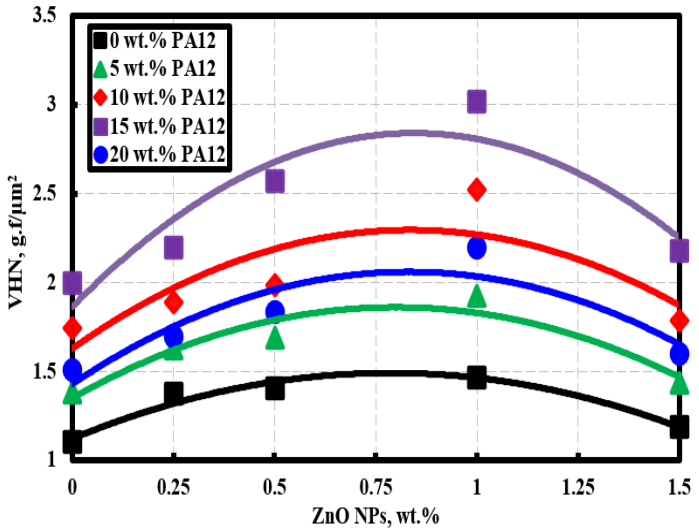

Fig. 6 Microhardness numbers of the present nanocomposites.

Figure 6 displays the microhardness results of the present PTFE/PA12/ZnO NPs composites. It is obvious that the microhardness measurements of the PTFE/PA12/ZnO NPs composites are higher than that of the unfilled PTFE. PA12 increased the microhardness of the pure PTFE by 25.19, 58.57, 81.68, and 36.82 % at 5, 10, 15, and 20 wt.% loadings, respectively. The best microhardness results of the PTFE/PA12 dual-matrix were achieved at 15 wt. % PA12, after which the VHN started to decrease. This may be due to the PA12 reinforced PTFE and thus improved the surface properties of the PTFE/PA12 dual-matrix. After incorporating 0.25, 0.5, 1, and 1.5 wt. % ZnO NPs into the PTFE/15 wt. % PA12, the VHN improved by 9.9, 28.61, 50.86, and 8.84 %, respectively. This may be because of the strong interfacial bonding between the ZnO NPs and the dual-matrix of PTFE/15 wt. % PA12 is achieved at 1 wt. % loading content. Moreover, ZnO NPs act as a strengthening filler of PTFE/PA12 composites that contribute to enhancement in load carrying capacity. Furthermore, the homogenous distribution of the nanofillers within the composites also plays an effective role in improving the surface mechanical properties, [48]. Thus, as indicated in Fig. 10 b, the uniform distribution of 1 wt. % ZnO NPs within the PTFE/15 wt. % PA12 was observed that led to enhancement of the VHN. After increasing ZnO NPs up to 1.5 wt. %, VHN gradually decreased. This may be due to the poor uniform distribution of ZnO NPs within the PTFE/PA12, which led to the formation of agglomerations and porosity into the composites, as indicated by SEM image, Fig. 10 e.

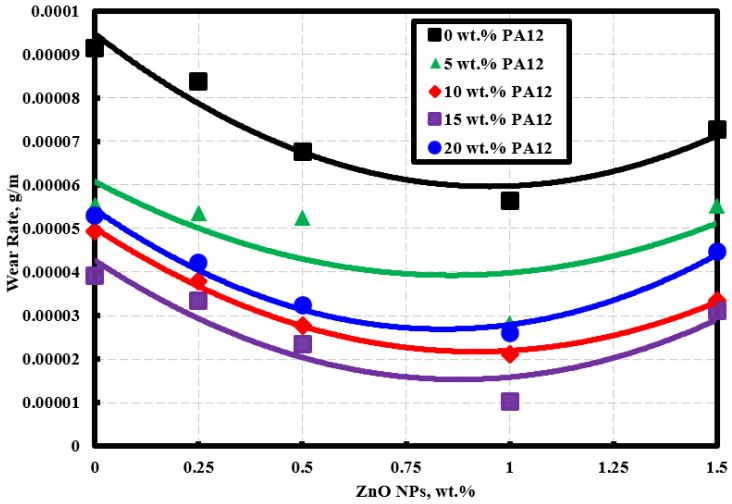

Fig. 7 Wear rate of the present nanocomposites.

The tribological tests, which include wear rate and friction coefficient were performed under applied normal load, sliding distance, and sliding speed of 30 N, 212 m, and 1.2 m/s, respectively. Figure 7 indicates the wear rate as a function of ZnO NPs loading content under dry sliding conditions. The pure PTFE recorded the highest wear rate value compared to PTFE/ZnO NPs at all loading content of PA12. Wear resistance of PTFE was enhanced by 8.35, 26, 38.28, and 20.53 % at ZnO NPs loadings of 0.25, 0.5, 1, and 1.5 wt. %, respectively. Consequently, the lowest wear rate achieved at 1 wt. % ZnO NPs. This may be due to the good strength and thermal conductivity of ZnO NPs, which improved the wear resistance of the composites at the rubbing surfaces, [49]. Also, the wear rate decreased gradually with an increase in the PA12 content up to 15 wt. %. Therefore, the wear rate of PTFE/15 wt. % PA12 dual-matrix decreased by 57.27 % compared to unfilled PTFE. After increasing the PA12 content up to 20 wt. %, the wear rate behavior trend began to increase compared to at 15 wt. % PA12. The reason for this is probably because the dual-matrix of PTFE/PA12 became completely saturated at 15 wt. % PA12. Moreover, after adding 1wt. % ZnO NPs to the dual-matrix of PTFE/15 wt. % PA12, the wear rate decreased significantly by 73.91 % compared to the double matrix without ZnO NPs. According to Archard equation, there is a relationship between the hardness number and wear rate of the composites, [50]. Therefore, the PTFE/15 wt. % PA12/1 wt. % ZnO NPs composites achieved the highest hardness number and thus had the lowest wear rate. When ZnO NPs content was increased up to 1.5 wt. %, the wear rate behavior trend started to increase compared to the 1 wt. % content. This may be due to the poor distribution of the ZnO NPs as well as their agglomerations within the composites. Finally, the composites of PTFE/15 wt. % PA12/1 wt. % ZnO NPs were the most suitable in prosthetic applications due to their wear resistance.

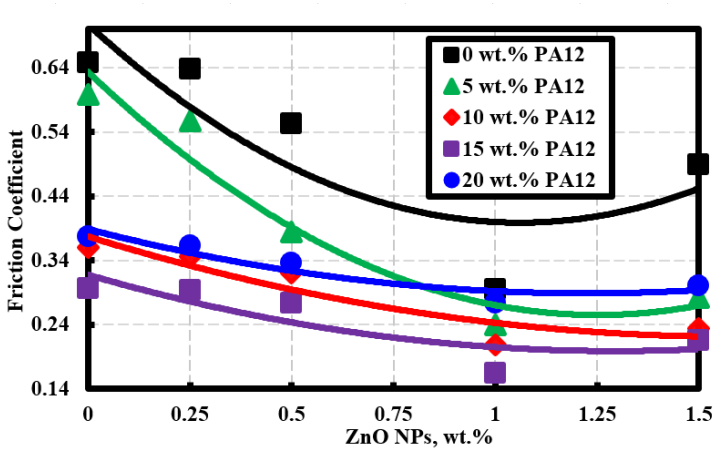

Fig. 8 Friction coefficient of the present nanocomposites.

The experimental results of friction coefficient versus ZnO NPs under dry sliding conditions were introduced in Fig. 8. It was declared that the pure PTFE records the largest friction coefficient value. By analyzing the results obtained, it may show that PA12 has a distinguished role to improve friction coefficient values of PTFE/PA12 dual-matrix. PA12 improved the friction coefficient of PTFE/PA12 dual-matrix by 7.67, 44.49, 54.16, and 41.69 % at 5, 10, 15, and 20 wt. % PA12 content, respectively compared to unfilled PTFE. Therefore, the dual-matrix of PTFE/15 wt. % PA12 showed the lowest friction coefficient value. According to the rule of mixtures, the friction coefficient is expected to decrease with increasing PA12 content up to 15 wt.%. It may be due to PA12 having higher strength than that of PTFE, which contributed to the improvement of the surface resistance to friction. Nevertheless, it can be noted that when the PA12 content was increased up to 20 wt. %, the friction coefficient behavior trend of the PTFE/PA12 dual-matrix began to increase. Moreover, ZnO NPs reduced the friction coefficient of pure PTFE by 1.54, 14.58, 54.51, and 24.47 % at 0.25, 0.5, 1, and 1.5 wt. % ZnO NPs content, respectively. Also, for the optimum dual-matrix of PTFE/15 wt. % PA12, the friction coefficient was significantly improved by 1.22, 7.83, 44.63, and 27.17 % at 0.25, 0.5, 1, and 1.5 wt. % ZnO NPs content, respectively. It can be noted that the best friction coefficient values were recorded at 1 wt. % ZnO NPs content for unfilled PTFE and all dual-matrices. This may be attributed to the uniform distribution of ZnO NPs within the composites achieved at 1 wt. % content. Numerous studies emphasized that the significant enhancement in tribological characteristics of polymer matrix nanocomposites may be due to the transfer film formation between rubbing surfaces. These films were responsible for protecting the asperities counterpart and specimens, leading to reducing the wear rate and friction coefficient, [51 - 54]. In consideration of the improved tribological properties, PTFE/15 wt. % PA12/1 wt. % ZnO NPs could be a promising composite for prosthetics applications. Summary of improvement percentages in the studied mechanical and tribological properties of the present dual-matrices and their reinforcement with ZnO NPs were shown in Figs 9, a and b, respectively.

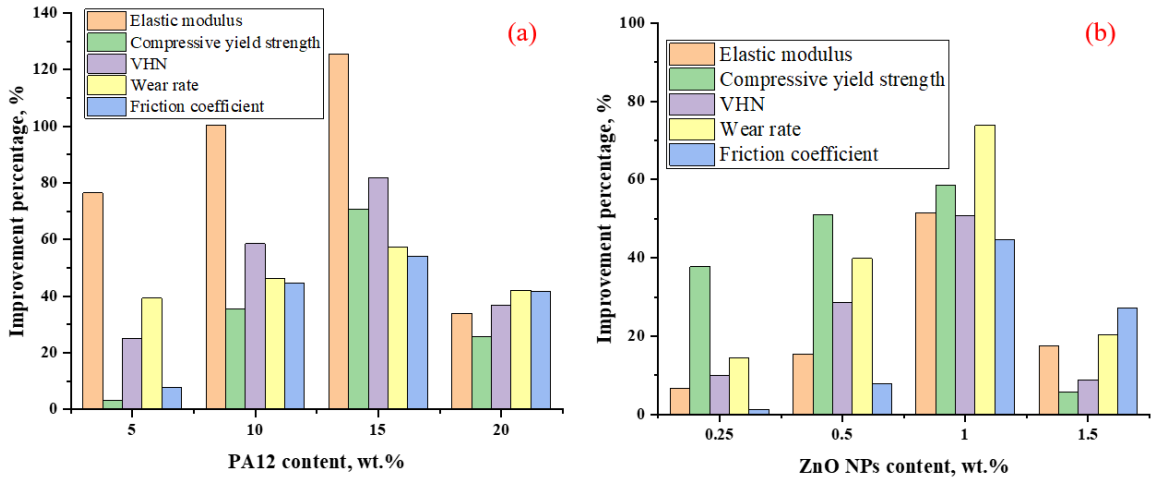

Fig. 9 Summery of improvement percentages in the mechanical and tribological properties. a), compared to unfilled PMMA, and b), compared to pure PTFE/15 wt. % PA12.

To examine the wear mechanisms, worn surfaces of the unfilled PTFE, PTFE/15 wt. % PA12/1 wt. % ZnO NPs, PTFE/20 wt. % PA12/1 wt. % ZnO NPs, and PTFE/15 wt. % PA12/1.5 wt. % ZnO NPs were imaged by SEM as indicated in Fig. 10. SEM observations revealed that the rubbed surfaces morphology varied according to the filler content. As shown in Fig. 10 a, the worn surface of the pure PTFE is characterized by many ploughed marks, delamination layers, voids, and grooves. Moreover, the weak layers removed from the rubbed surface led to an increase in shear resistance and, consequently, the friction coefficient, [47]. For this reason, the results of the wear rate and friction coefficient of the unfilled PTFE deteriorated. Therefore, the wear mechanism for unfilled PTFE sample was distinguished with ploughing and abrasive wear.

The worn surface morphology details of PTFE/15 wt. % PA12/1 wt. % ZnO NPs sample, instead, appeared smoother than that of the pure PTFE, as shown in Fig. 10, c. This can be attributed to the improvement in the surface properties and strength after increasing the PA12 up to 15 wt. % and ZnO NPs up to 1 wt. %. Also, the transfer films, which were formed between the rubbed surfaces play a significant role in enhancing the wear characteristics of the material, [55]. During the wear test, the formed transfer film, which contains rubbed debris released from the sample was transferred between the sample contact zone and the abrasive counterface. Thus, the transfer film prevented the abrasive disc asperities from penetrating into the sample. Therefore, the worn surface of the PTFE/15 wt. % PA12/1 wt. % ZnO NPs nanocomposite appeared to contain very few wear marks compared to the pure PTFE. Hence the wear rate and friction coefficient were enhanced.

Worn surfaces of PTFE/20 wt. % PA12/1 wt. % ZnO NPs and PTFE/15 wt. % PA12/1.5 wt. % ZnO NPs nanocomposites were shown in Figs 10 d and e, respectively. As shown in Figs 10 d and e, the worn surfaces that were observed contain more ploughed and wear marks than the PTFE/15 wt. % PA12/1 wt. % ZnO NPs sample. This may be attributed to the poor surface mechanical properties due to the formation

of porosity resulting from agglomeration of the nanofiller. These observations are compatible with the mechanical and tribological properties of the PTFE/20 wt. % PA12/1 wt. % ZnO NPs and PTFE/15 wt. % PA12/1.5 wt. % ZnO NPs composites.

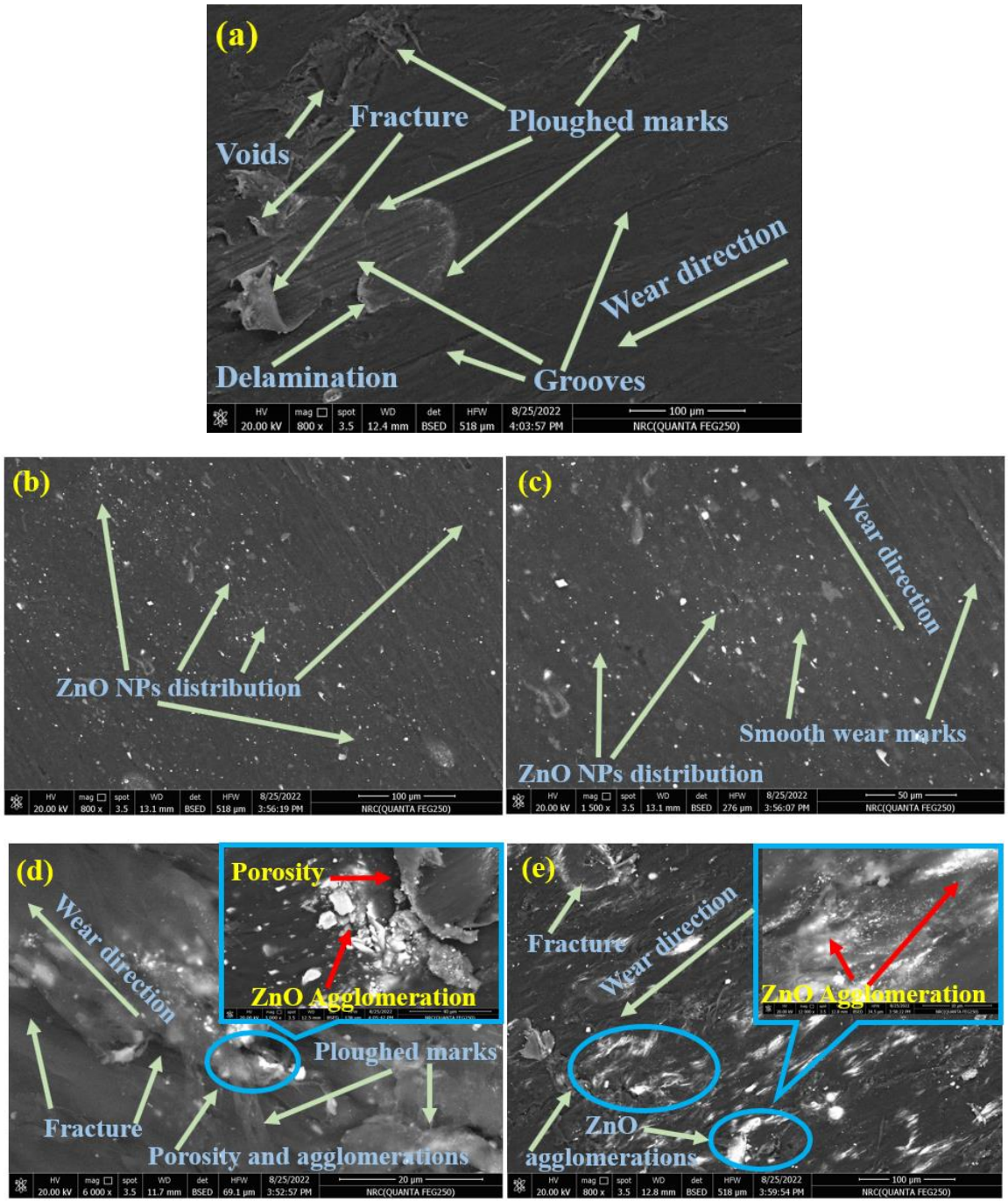

Fig. 10 SEM micrographs. a): worn surface of unfilled PTFE after wear, b): distribution of 1 wt. % ZnO NPs in PTFE/15 wt. % PA12 before wear, c): worn surface of PTFE/15 wt.% PA12/1 wt. % ZnO NPs after wear, d): worn surface of PTFE/20 wt. % PA12/1 wt. % ZnO NPs after wear, and e): worn surface of PTFE/15 wt. % PA12/1.5 wt. % ZnO NPs after wear.

CONCLUSIONS

In the current study, PTFE was reinforced with PA12 at 5, 10, 15, and 20 wt. % to fabricate a polymeric dual-matrix. The dual-matrix was reinforced with 0.25, 0.5, 1, and 1.5 wt. % ZnO NPs to obtain PTFE/PA12/ZnO NPs composites. It was concluded that PTFE could be successfully reinforced by 15 wt.% PA12 content. Elastic modulus, compressive yield strength, VHN, wear rate, and friction coefficient of PTFE/15 wt. % PA12 dual-matrix were enhanced by 125.48, 70.88, 81.68, 57.27, and 54.16 %, respectively compared to the pure PTFE. After reinforcing the dual-matrix of PTFE/15 wt.% PA12 with 1 wt.% of ZnO NPs, elastic modulus, compression yield strength, VHN, wear rate, and friction coefficient of the new composite showed a significant improvement by 51.58, 58.59, 50.86, 73.91, and 44.63%, respectively compared to the pure dual-matrix. Also, a significant enhancement in the worn surface occurred after addition of 1 wt.% ZnO NPs to the dual matrix of PTFE/15 wt.% PA12 compared to the other tested worn surfaces. Therefore, the proposed nanocomposites of PTFE/15 wt.% PA12/1 wt.% ZnO NPs are considered as a suitable choice for prosthetic applications.

ACKNOWLEDGEMENTS

This work was supported by materials lab, production technology department, faculty of technology and education, Beni-Suef University, Egypt.

REFERENCES

1. W. K. Chee, H. N. Lim, N. M. Huang, and I. Harrison, "Nanocomposites of graphene/polymers: a review," RSC Adv., vol. 5, no. 83, pp. 68014–68051, (2015)

2. Y. Zhao et al., "Progressive macromolecular self-assembly: From biomimetic chemistry to bio-inspired materials," Adv. Mater., vol. 25, no. 37, pp. 5215–5256, (2013).

3. A. M. Alosaimi et al., "Recent Biomedical Applications of Coupling Nanocomposite Polymeric Materials Reinforced with Variable Carbon Nanofillers," Biomedicines, vol. 11, no. 3, (2023).

4. T. Aida, E. W. Meijer, and S. I. Stupp, "Functional supramolecular polymers," Science (80-.)., vol. 335, no. 6070, pp. 813–817, (2012).

5. B. J. Briscoe and S. K. Sinha, Tribological applications of polymers and their composites - past, present and future prospects, Second Edi. Elsevier, (2013)

6. S. Sinha Ray, "Polylactide-based bionanocomposites: A promising class of hybrid materials," Acc. Chem. Res., vol. 45, no. 10, pp. 1710–1720, (2012).

7. S. M. Liff, N. Kumar, and G. H. McKinley, "High-performance elastomeric nanocomposites via solvent-exchange processing," Nat. Mater., vol. 6, no. 1, pp. 76–83, (2007).

8. A. K. Gaharwar, S. A. Dammu, J. M. Canter, C. J. Wu, and G. Schmidt, "Highly extensible, tough, and elastomeric nanocomposite hydrogels from poly(ethylene glycol) and hydroxyapatite nanoparticles," Biomacromolecules, vol. 12, no. 5, pp. 1641–1650, (2011).

9. D. R. Paul and L. M. Robeson, "Polymer nanotechnology: Nanocomposites," Polymer (Guildf)., vol. 49, no. 15, pp. 3187–3204, (2008).

10. L. C. Seabra and A. M. Baptista, "Tribological behaviour of food grade polymers against stainless steel in dry sliding and with sugar," Wear, vol. 253, no. 3–4, pp. 394–402, (2002).

11. T. W. Scharf and S. V. Prasad, "Solid lubricants: A review," J. Mater. Sci., vol. 48, no. 2, pp. 511–531, (2013).
12. G. Zhao, I. Hussainova, M. Antonov, Q. Wang, and T. Wang, "Friction and wear of fiber reinforced polyimide composites," Wear, vol. 301, no. 1–2, pp. 122–129, (2013).
13. X. Feng, H. Wang, Y. Shi, D. Chen, and X. Lu, "The effects of the size and content of potassium titanate whiskers on the properties of PTW/PTFE composites," Mater. Sci. Eng. A, vol. 448, no. 1–2, pp. 253–258, 2007, doi: 10.1016/j.msea., (2006).
14. X. Feng, X. Diao, Y. Shi, H. Wang, S. Sun, and X. Lu, "A study on the friction and wear behavior of polytetrafluoroethylene filled with potassium titanate whiskers," Wear, vol. 261, no. 11–12, pp. 1208–1212, (2006).
15. Z. Jiang et al., "Direct Ink Writing of Poly(tetrafluoroethylene) (PTFE) with Tunable Mechanical Properties," ACS Appl. Mater. Interfaces, vol. 11, no. 31, pp. 28289–28295, (2019).
16. Y. Shi, X. Feng, H. Wang, and X. Lu, "The effect of surface modification on the friction and wear behavior of carbon nanofiber-filled PTFE composites," Wear, vol. 264, no. 11–12, pp. 934–939, (2008).
17. J. Zhu, Y. Shi, X. Feng, H. Wang, and X. Lu, "Prediction on tribological properties of carbon fiber and TiO2 synergistic reinforced polytetrafluoroethylene composites with artificial neural networks," Mater. Des., vol. 30, no. 4, pp. 1042–1049, (2009).
18. X. L. Liwen Mu, Jian Chen, Yijun Shi, Xin Feng, Jiahua Zhu, Huaiyuan Wang, "Durable polytetrafluoroethylene composites in harsh environments: tribology and corrosion investigation," J. Appl. Polym. Sci., vol. 124, no. 5, pp. 4307–4314, (2012).
19. Y. Shi, L. Mu, X. Feng, and X. Lu, "The tribological behavior of nanometer and micrometer TiO2 particle-filled polytetrafluoroethylene/polyimide," Mater. Des., vol. 32, no. 2, pp. 964–970, (2011).
20. D. L. Burris and W. G. Sawyer, "A low friction and ultra low wear rate PEEK/PTFE composite," Wear, vol. 261, no. 3–4, pp. 410–418, 2006, doi: 10.1016/j.wear, (2005).
21. B. A. Stachowiak GW, "16- Wear of non-metallic materials," Eng. Tribol. Third Ed, Elsevier Butterworth-Heinemann, Burlingt., pp. 651–704, (2006).
22. M. Arhant, P. Y. Le Gac, M. Le Gall, C. Burtin, C. Briançon, and P. Davies, "Modelling the non Fickian water absorption in polyamide 6," Polym. Degrad. Stab., vol. 133, no. November, pp. 404–412, (2016).
23. J. Diani and K. Gall, "Finite Strain 3D Thermoviscoelastic Constitutive Model," Society, pp. 1–10, (2006).
24. A. Touris et al., "Effect of molecular weight and hydration on the tensile properties of polyamide 12," Results Mater., vol. 8, no. September, p. 100149, (2020).
25. T. S. Ghanta, "Review on nano-and microfiller-based polyamide 6 hybrid composite : Effect on mechanical properties and morphology," no. October 2019, pp. 1–43, (2020).
26. A. Pogačnik, A. Kupec, and M. Kalin, "Tribological properties of polyamide (PA6) in self-mated contacts and against steel as a stationary and moving body," Wear, vol. 378–379, pp. 17–26, (2017).
27. F. He, B. Liu, L. Chen, D. Guo, X. Ding, and Y. Xiao, "Novel polyamide 6 composites based on Schiff-base containing phosphonate oligomer : High flame retardancy , great processability and mechanical property," Compos. Part A, vol. 146, no. April, p. 106423, (2021).

28. Y. Shi, S. Zhou, H. Zou, M. Liang, and Y. Chen, "In situ micro-fibrillization and post annealing to significantly improve the tribological properties of polyphenylene sulfide/polyamide 66/polytetrafluoroethylene composites," Compos. Part B Eng., vol. 216, no. January, p. 108841, (2021).
29. Q. Xu, N. Zhang, W. Li, S. Zhang, and W. He, "Preparation of ZnO Nanoparticle-Reinforced Polyamide 6 Composite by In Situ -Coproduced Method and Their Properties," pp. 165–170, (2019).
30. S. M. Mohd Firdaus Omar, Hazizan Md Akil, Zainal Arifin Ahmad, "The Effect of Loading Rates and Particle Geometry on Compressive Properties of Polypropylene/Zinc Oxide Nanocomposites: Experimental and Numerical Prediction," Polym. Polym. Compos., vol. 33, no. 1, pp. 99–108, (2012).
31. D. Kaur, A. Bharti, T. Sharma, and C. Madhu, "Dielectric Properties of ZnO-Based Nanocomposites and Their Potential Applications," vol. 2021, (2021).
32. H. Chakraborty, A. Sinha, N. Mukherjee, D. Ray, and P. Protim Chattopadhyay, "A study on nanoindentation and tribological behaviour of multifunctional ZnO/PMMA nanocomposite," Mater. Lett., vol. 93, pp. 137–140, (2013).
33. B. P. Chang, H. M. Akil, R. B. M. Nasir, I. M. C. C. D. Bandara, and S. Rajapakse, "The effect of ZnO nanoparticles on the mechanical, tribological and antibacterial properties of ultra-high molecular weight polyethylene," J. Reinf. Plast. Compos., vol. 33, no. 7, pp. 674–686, (2014).
34. H. J. Song, Z. Z. Zhang, X. H. Men, and Z. Z. Luo, "A study of the tribological behavior of nano-ZnO-filled polyurethane composite coatings," Wear, vol. 269, no. 1–2, pp. 79–85, (2010).
35. L. Mu et al., "Self-lubricating polytetrafluoroethylene/polyimide blends reinforced with zinc oxide nanoparticles," J. Nanomater., vol. 2015, (2015).
36. F. Li, K. ao Hu, J. lin Li, and B. yuan Zhao, "The friction and wear characteristics of nanometer ZnO filled polytetrafluoroethylene," Wear, vol. 249, no. 10–11, pp. 877–882, (2001).
37. A. M. Díez-Pascual, C. Xu, and R. Luque, "Development and characterization of novel poly(ether ether ketone)/ZnO bionanocomposites," J. Mater. Chem. B, vol. 2, no. 20, pp. 3065–3078, (2014).
38. Q. Xu, N. Zhang, W. Li, S. Zhang, and W. He, "Preparation of ZnO Nanoparticle-Reinforced Polyamide 6 Composite by In Situ -Coproduced Method and Their Properties," pp. 1–6, (2018).
39. K. Saeed et al., "Preparation of ZnO / Nylon 6 / 6 nanocomposites , their characterization and application in dye decolorization," Appl. Water Sci., vol. 11, no. 6, pp. 1–10, (2021).
40. R. O. Medupin, O. K. Abubakre, and A. S. Abdulkareem, "Carbon Nanotube Reinforced Natural Rubber Nanocomposite for Anthropomorphic Prosthetic Foot Purpose," pp. 1–11, (2019).
41. S. Dabees, B. M. Kamel, V. Tirth, and A. B. Elshalakny, "Experimental design of Al 2 O 3 / MWCNT / HDPE hybrid nanocomposites for hip joint replacement," Bioengineered, vol. 11, no. 1, pp. 679–692, (2020).
42. Y. H. Dds and K. Nakajima, "ScienceDirect Application of Ce-TZP / Al 2 O 3 nanocomposite to the framework of an implant-fixed complete dental prosthesis and a complete denture," J. Prosthodont. Res., pp. 1–7, (2016).
43. A. E.-S. M. Hassan, A. I. EiD, M. El-Sheikh, and W. Y. Ali, "Effect of Graphene Nanoplatelets and Paraffin Oil Addition on the Mechanical and Tribological

Properties of Low-Density Polyethylene Nanocomposites," Arab. J. Sci. Eng., vol. 43, no. 3, pp. 1435–1443, (2018).
44. A. El-sayed Mohamed Hassan, M. Naguib El-sheikh, W. Yosry Ali, and M. Nafea Metwally Rohim, "Mechanical and Tribological Performance of Self-Cured Poly Methyl Methacrylate Reinforced by Alumina Nanowires and Zirconia Nanoparticles for Denture Applications," Mater. Plast, vol. 58, no. 3, pp. 109–120, (2021).
45. A. E. M. Hassan, A. I. EiD, M. El-Sheikh, and W. Y. Ali, "Mechanical and tribological performance of polyamide 12 reinforced with graphene nanoplatelets and paraffin oil nanocomposites," Materwiss. Werksttech., vol. 50, no. 1, pp. 74–85, (2019).
46. B. Aramide, S. Pityana, R. Sadiku, T. Jamiru, and P. Popoola, "Improving the durability of tillage tools through surface modification—a review," Int. J. Adv. Manuf. Technol., vol. 116, no. 1–2, pp. 83–98, (2021).
47. A. Nabhan, M. Taha, and N. M. Ghazaly, "Filler loading effect of Al2O3/TiO2 nanoparticles on physical and mechanical characteristics of dental base composite (PMMA)," Polym. Test., vol. 117, no. October 2022, p. 107848, (2023).
48. H. J. Park, S. Y. Kwak, and S. Kwak, "Wear-resistant ultra high molecular weight polyethylene/zirconia composites prepared by in situ ziegler-natta polymerization," Macromol. Chem. Phys., vol. 206, no. 9, pp. 945–950, (2005).
49. B. Pan et al., "Tribological and mechanical investigation of MC nylon reinforced by modified graphene oxide," Wear, vol. 294–295, pp. 395–401, (2012).
50. E. Hornbogen, "Role of Fracture Toughness in the Wear of Metals.," Wear, vol. 33, no. 2, pp. 251–259, (1975).
51. B. Peng Chang, H. Md Akil, R. Bt Nasir, and A. Khan, "Optimization on wear performance of UHMWPE composites using response surface methodology," Tribol. Int., vol. 88, pp. 252–262, (2015).
52. C. Guo, L. Zhou, and J. Lv, "Influence of Solid Lubricant Reinforcement on Wear Behavior of Kevlar Fabric Composites," Appl. Polym. Sci., vol. 110, pp. 1771–1777, (2008).
53. Y. Li, Q. Wang, T. Wang, and G. Pan, "Preparation and tribological properties of graphene oxide/nitrile rubber nanocomposites," J. Mater. Sci., vol. 47, no. 2, pp. 730–738, (2012).
54. H. Liu, Y. Li, T. Wang, and Q. Wang, "In situ synthesis and thermal, tribological properties of thermosetting polyimide/graphene oxide nanocomposites," J. Mater. Sci., vol. 47, no. 4, pp. 1867–1874, (2012).
55. B. P. Chang, H. M. Akil, M. G. Affendy, A. Khan, and R. B. M. Nasir, "Comparative study of wear performance of particulate and fiber-reinforced nano-ZnO/ultra-high molecular weight polyethylene hybrid composites using response surface methodology," Mater. Des., vol. 63, pp. 805–819, (2014).